Weierstraß–Institut
für Angewandte Analysis und Stochastik

im Forschungsverbund Berlin e.V.

Preprint ISSN 0946 – 8633

On the approximation of kinetic equations by moment systems

Wolfgang Dreyer[1], Michael Junk[2], Matthias Kunik[1]

submitted: 27th June 2000

[1] Weierstrass Institute
for Applied Analysis
and Stochastics
Mohrenstraße 39
D – 10117 Berlin
Germany
E-Mail: dreyer@wias-berlin.de
E-Mail: kunik@wias-berlin.de

[2] FB Mathematik
Universität Kaiserslautern
Erwin-Schrödinger-Straße
D – 67663 Kaiserslautern
Germany
E-Mail: junk@mathematik.uni-kl.de

Preprint No. 592
Berlin 2000

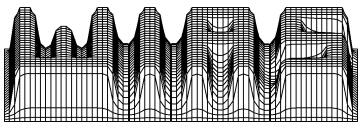

2000 *Mathematics Subject Classification.* 82C70, 35L30, 82B40.

Key words and phrases. maximum entropy, moment methods, Fokker-Planck equation, exact solution, Grad expansion, moment realizability.

Edited by
Weierstraß–Institut für Angewandte Analysis und Stochastik (WIAS)
Mohrenstraße 39
D — 10117 Berlin
Germany

Fax: + 49 30 2044975
E-Mail (X.400): c=de;a=d400-gw;p=WIAS-BERLIN;s=preprint
E-Mail (Internet): preprint@wias-berlin.de
World Wide Web: http://www.wias-berlin.de/

Abstract

The aim of this article is to show that moment approximations of kinetic equations based on a Maximum Entropy approach can suffer from severe drawbacks if the kinetic velocity space is unbounded. As example, we study the Fokker Planck equation where explicit expressions for the moments of solutions to Riemann problems can be derived. The quality of the closure relation obtained from the Maximum Entropy approach as well as the Hermite/Grad approach is studied in the case of five moments. It turns out that the Maximum Entropy closure is even singular in equilibrium states while the Hermite/Grad closure behaves reasonably. In particular, the admissible moments may lead to arbitrary large speeds of propagation, even for initial data arbitrary close to global eqilibrium.

Keywords. maximum entropy, moment methods, Fokker-Planck equation, exact solution, Grad expansion, moment realizability

1 Introduction

1.1 Objectives of this study

In this article, we study both the Maximum Entropy method and the HERMITE/GRAD approach as moment approximations of the FOKKER PLANCK equation.

There are several advantages in the Maximum Entropy approach like non-negativity of distribution functions and global symmetric hyperbolicity which are in general not achieved with expansion methods like the HERMITE/GRAD approach. Moreover, the HERMITE/GRAD system can be identified with a linearization of the *Maximum Entropy system* which seems to indicate that the approach based on the Maximum Entropy Principle is superior to the GRAD expansion method.

Our main objective is to show that this impression is *not* justified.

These observations also apply to more general cases: whenever the velocity space in the underlying kinetic equation is unbounded, when the entropy functional is essentially given by $H(f) = -\int_{\mathbb{R}^d} f \log f \, d\mathbf{c}$, when equilibrium states are related to Maxwellian distributions and when velocity moments of order four and higher are used (these assumptions are satisfied for the FOKKER PLANCK equation but also for the BOLTZMANN equation of gas dynamics or the semiconductor BOLTZMANN equation with parabolic bands). It turns out that in such cases the equilibrium

states are located on the boundary of the domain of definition of the *Maximum Entropy system*. Moreover, the flux is singular in these states which leads to a very unexpected behavior of the systems. Note that there are kinetic equations and corresponding entropy functionals where these problems do not appear. One example is the kinetic model of phonons as carriers of heat in crystals, see [4], [5].

Both complications do not arise in the HERMITE/GRAD approach which will lead to two conclusions: firstly, the GRAD system is a bad approximation of the *Maximum Entropy system* because the singular behavior is not captured. Secondly, the GRAD system is in better coincidence with the FOKKER PLANCK equation. Thus, despite of the disadvantages concerning positivity of even moments and hyperbolicity, the HERMITE/GRAD system seems to be favorable.

We conclude the introduction with an outline of the article. In the remaining sections of the first chapter, we introduce the FOKKER PLANCK equation as well as the basic moment approximations. In the second chapter, we then construct explicit solutions of the Cauchy problem for the FOKKER PLANCK equation and give analytic formulas for the first five moments of the solution with RIEMANN initial data. In chapter 3, the *Maximum Entropy system* is studied in more detail with respect to its domain of definition and the singular behavior of the flux. In the last chapter, the approximation properties of both the HERMITE/GRAD and the Maximum Entropy approach are investigated.

1.2 Brownian motion and the Fokker Planck equation

In 1827 the English botanist ROBERT BROWN studied macroscopically small but microscopically large particles that are suspended in a liquid. He observed that the particles perform a steady irregular motion. Today this phenomenon is called BROWNian motion and the particles are called BROWNian particles. Soon after its discovery, it became evident that BROWNian motion is caused by the interaction of BROWNian particles with the liquid molecules which are permanently in thermal motion. At room temperature a BROWNian particle suffers about 10^{21} collisions per second with the liquid molecules and this can be considered as a continuous interaction process. For details see [2]. A BROWNian particle with an initial speed being larger than the thermal velocity $\sqrt{(k/m)\,T}$, is slowed down to the thermal value, while it is accelerated to the thermal velocity when it has initially a smaller speed than $\sqrt{(k/m)\,T}$. Here T is the (absolute) temperature of the liquid, m is the mass of the BROWNian particle, and k denotes the BOLTZMANN constant.

The quantitative description of BROWNian motion started in 1905 with a series of papers by ALBERT EINSTEIN, see for example [6], [7] and his investigations finally leads to the formulation of the FOKKER PLANCK equation which serves in our study as the kinetic model.

The central quantity of the kinetic model is the function $W : \mathbb{R}_0^+ \times \mathbb{R}^d \times \mathbb{R}^d \to \mathbb{R}_0^+$, d=1,2,3, which is the phase density of BROWNian particles. Physically speaking, $W(t, \mathbf{x}, \mathbf{c})$ is the number density of BROWNian particles in the vicinity of the phase point $(\mathbf{x}, \mathbf{c})$ at time t. We will assume that the BROWNian particles are contained in a liquid at rest and at constant temperature T, which is not set into motion by the motion of the BROWN ian particles. Furthermore, we neglect interaction among the particles and do not consider external forces. In this case, the evolution of the phase density W is determined by the FOKKER PLANCK equation, see [2],

$$\frac{\partial W}{\partial t} + c_k \frac{\partial W}{\partial x_k} = \frac{1}{\tau} \frac{\partial}{\partial c_k} \left(c_k W + \left(\frac{k}{m} T \right) \frac{\partial W}{\partial c_k} \right). \tag{1}$$

The positive quantity τ is a relaxation time, and A. EINSTEIN showed that τ is related to the diffusion constant D and the viscosity η of the liquid by the famous relations

$$m/\tau = \frac{k\,T}{D} = 6\pi\eta a\,,$$

see [6], [7]. The positive constant a is the radius of the Brownian particle.

In the following, we will work with a scaled version of (1) by going over to new time, space, and velocity coordinates $(\bar{t}, \bar{x}, \bar{c})$ according to $t = \tau\bar{t}$, $x = \tau\sqrt{(k/m)T}\bar{x}$, $c = \sqrt{(k/m)T}\bar{c}$. After dropping the bar superscripts, we end up with the FOKKER PLANCK equation in dimensionless coordinates

$$\frac{\partial W}{\partial t} + c_k \frac{\partial W}{\partial x_k} = \frac{\partial}{\partial c_k} \left(c_k W + \frac{\partial W}{\partial c_k} \right). \tag{2}$$

For theoretical investigations of equation (2), we refer to the articles of [2] and [15].

1.3 General equations of transfer and H-theorem

Based on the phase density W, other important physical quantities can be derived by taking velocity moments. For example, the number density $n : \mathbb{R}_0^+ \times \mathbb{R}^d \to \mathbb{R}_0^+$ is given by

$$n(t, \mathbf{x}) = \int_{\mathbb{R}^d} W(t, \mathbf{x}, \mathbf{c})\, d\mathbf{c}. \tag{3}$$

More generally, any function $\psi : \mathbb{R}_0^+ \times \mathbb{R}^d \times \mathbb{R}^d \to \mathbb{R}$ gives rise to the mean value

$$\langle \psi \rangle (t, \mathbf{x}) = \frac{1}{n(t, \mathbf{x})} \int_{\mathbb{R}^d} \psi(t, \mathbf{x}, \mathbf{c})\, W(t, \mathbf{x}, \mathbf{c})\, d\mathbf{c}. \tag{4}$$

In the following, we assume that the phase space density W decays sufficiently fast for all appearing $\mathbf{c}$-integrals to be valid. This will certainly be satisfied for the solutions of (2) which we construct in section 2.

The FOKKER PLANCK equation implies a balance equation for $n\langle\psi\rangle$

$$\frac{\partial n\langle\psi\rangle}{\partial t}+\frac{\partial n\langle\psi c_k\rangle}{\partial x_k}=E_\psi+C_\psi. \tag{5}$$

The production density on the right hand side of the balance equation consists of two contributions, viz.

$$E_\psi=n\left\langle\frac{\partial\psi}{\partial t}+c_k\frac{\partial\psi}{\partial x_k}\right\rangle \quad\text{and}\quad C_\psi=\int_{\mathbb{R}^d}\psi\frac{\partial}{\partial c_k}\left(c_kW+\frac{\partial W}{\partial c_k}\right)d\mathbf{c}. \tag{6}$$

These contributions are called *eigen production* and *collision production*, respectively. The collision production can be represented by two alternative but equivalent forms:

$$C_\psi=-\int_{\mathbb{R}^d}\left(c_kW+\frac{\partial W}{\partial c_k}\right)\frac{\partial\psi}{\partial c_k}d\mathbf{c}=-\int_{\mathbb{R}^d}W\frac{\partial\log\left(\frac{W}{W^{eq}}\right)}{\partial c_k}\frac{\partial\psi}{\partial c_k}d\mathbf{c}. \tag{7}$$

Here, the newly introduced function W^{eq} is the standard MAXWELLian distribution function which is defined by

$$W^{eq}\left(\mathbf{c}\right)=\frac{1}{(2\pi)^{\frac{d}{2}}}\exp\left(-\frac{|\mathbf{c}|^2}{2}\right). \tag{8}$$

In section 1.4.1 and 1.4.3 we will consider special choices for the generic function ψ that will lead to moment systems relying on (5). To this end the first alternative of (7) will become useful. The second alternative of (7) will be used now to establish the *H-theorem*. We choose

$$\psi\left(t,\mathbf{x},\mathbf{c}\right)=-\log\left(\frac{W\left(t,\mathbf{x},\mathbf{c}\right)}{W^{eq}\left(\mathbf{c}\right)}\right), \tag{9}$$

and define entropy density, h, and entropy flux, φ_k, of the Brownian particles according to

$$\begin{aligned}h\left(t,x\right)&=-\int_{\mathbb{R}^d}W\left(t,\mathbf{x},\mathbf{c}\right)\log\left(\frac{W\left(t,\mathbf{x},\mathbf{c}\right)}{W^{eq}\left(\mathbf{c}\right)}\right)d\mathbf{c},\\ \varphi_k\left(t,x\right)&=-\int_{\mathbb{R}^d}c_kW\left(t,\mathbf{x},\mathbf{c}\right)\log\left(\frac{W\left(t,\mathbf{x},\mathbf{c}\right)}{W^{eq}\left(\mathbf{c}\right)}\right)d\mathbf{c}.\end{aligned} \tag{10}$$

With these definitions we obtain from (5) the *entropy inequality*

$$\frac{\partial h}{\partial t}+\frac{\partial\varphi_k}{\partial x_k}=\int_{\mathbb{R}^d}W\frac{\partial\log\left(\frac{W}{W^{eq}}\right)}{\partial c_k}\frac{\partial\log\left(\frac{W}{W^{eq}}\right)}{\partial c_k}d\mathbf{c}\geq 0. \tag{11}$$

The right hand side of the entropy inequality gives the entropy production which is non-negative. The entropy production is zero only if $W=nW^{eq}$ for some $\mathbf{c}$ independent $n\in\mathbb{R}^+$. This statement establishes the H-theorem for BROWNian particles. Since equilibrium is defined as a process where the entropy production vanishes, we conclude that in global equilibrium, the distribution of BROWNian particles is a MAXWELLian distribution.

1.4 Moment systems of the Fokker Planck equation

For simplicity, we consider from now on the one-dimensional model problem $d = 1$ exclusively.

In thermodynamics the phase density is not the quantity of primary interest. Here the main objective is the solution of initial and boundary value problems for the velocity first moments. For this reason thermodynamicists do not consider the Fokker Planck equation by itself, rather they consider the equations of balance for the moments as the basic equations.

Assuming that, for some $M \in \mathbb{N}$, the function $c \mapsto W(t,x,c)$ is contained in the set

$$\mathcal{W}_M = \{W \in \mathbb{L}^1(\mathbb{R}) : c \mapsto |c|^{M-1} W(c) \in \mathbb{L}^1(\mathbb{R}), W \geq 0\} \tag{12}$$

we introduce the (ordinary) moments

$$u_A(t,x) = \int_{-\infty}^{\infty} c^A W(t,x,c)\, dc, \quad A = 0,1,2,...,M-1. \tag{13}$$

To express the dependence of the moments $\mathbf{u} = (u_0, u_1, ..., u_{M-1})$ on the phase density, we sometimes use the notation $\mathbf{u} = \boldsymbol{\mu}^{(M)}(W)$. Note that the first four moments have a direct physical interpretation: $u_0 = n$ is the number density of Brownian particles, $u_1 = nv$ is their momentum density with v being the velocity, $u_2/2$ is the energy density, and $u_3/2-$ is the energy flux.

The balance equations for the moments are easily obtained from (5) for the choice $\psi(t, \mathbf{x}, \mathbf{c}) \in \{1, c, c^2, ...\}$

$$\frac{\partial u_A}{\partial t} + \frac{\partial u_{A+1}}{\partial x} = P_A, \quad with \quad P_A = -A u_A + A(A-1) u_{A-2}. \tag{14}$$

We conclude that these equations form an infinite hierarchy of coupled equations. If we pose an initial value problem for the first M moments $u_0, u_1, ..., u_{M-1}$ as the variables, then the balance equation for the highest moment u_{M-1} contains the flux u_M which does not occur among the variables and we are confronted with a *closure problem.*

In thermodynamics the closure problem is solved by two **assumptions:** (i) the thermodynamic state of the process under consideration is sufficiently described by the first M moments as variables, where M depends on the degree of deviation of the considered process from equilibrium, (ii) the highest moment u_M is given by a function $F : \mathbb{R}^M \to \mathbb{R}$ of the variables, and we write

$$u_M = F(u_0, u_1, ..., u_{M-1}). \tag{15}$$

There are many different strategies to derive expressions for the unknown function F. Two of these will be studied in detail now. In particular, we will answer the question,

whether the resulting moment systems (14) constitute reasonable approximations of the solution of the original FOKKER PLANCK equation. Both strategies rely on the assumption that the dependence of the phase density on time and space is in fact a dependence on the variables $\mathbf{u}(t,x)$

$$W(t,x,c) = \hat{W}(u_0(t,x), u_1(t,x), ..., u_{M-1}(t,x), c). \tag{16}$$

Note that, in view of (16) and (15), any such relation gives rise to a closure of the moment system.

1.4.1 The Maximum Entropy system

The determination of the function $\hat{W}$ by the *Maximum Entropy Principle* (MEP) relies on the requirement that, even in non-equilibrium, the phase density should maximize the entropy density under the constrained of prescribed values of of the M variables $u_0, u_1, ..., u_{M-1}$ (see for example [3]). More precisely, $\hat{W}(\mathbf{u}, c)$ is taken as solution of the problem

$$\max\{H(W) : W \in \mathcal{W}_M,\ \boldsymbol{\mu}^{(M)}(W) = \boldsymbol{u}\} \tag{17}$$

where H is the entropy density as a functional of the phase density

$$H(W) = -\int_{-\infty}^{\infty} W \log\left(\frac{W}{W^{eq}}\right) dc. \tag{18}$$

Note that $H(W(t,x,\cdot)) = h(t,x)$ as given in (10).

Formally, the solution of the constrained optimization problem (17) is obtained with the method of Lagrange multipliers. To this end, we introduce the Lagrange functional

$$\mathcal{L}(W, \boldsymbol{\lambda}) := H(W) + \boldsymbol{\lambda} \cdot (\boldsymbol{\mu}^{(M)}(W) - \boldsymbol{u}) \tag{19}$$

and maximize it with respect to W for fixed Lagrange multipliers $\boldsymbol{\lambda} \in \mathbb{R}^M$. Assuming that $W_{\boldsymbol{\lambda}}$ is an extremal point of $\mathcal{L}$, we get

$$0 = \delta\mathcal{L}(W_{\boldsymbol{\lambda}}, \boldsymbol{\lambda}) = \log W^{eq} - 1 - \log W_{\boldsymbol{\lambda}} + \sum_{A=0}^{M-1} \lambda_A c^A \tag{20}$$

so that

$$W_{\boldsymbol{\lambda}}(t,x,c) = W^{eq}(c) \exp\left(\sum_{A=0}^{M-1} \lambda_A(t,x) c^A - 1\right). \tag{21}$$

The elimination of the LAGRANGE multipliers by means of the constraints

$$u_A = \int_{-\infty}^{\infty} c^A W_{\boldsymbol{\lambda}} dc, \quad A \in \{0, 1, ..., M-1\} \tag{22}$$

leads to two important questions: (i) Do the integrals on the right hand side of (22) exist? (ii) Are the constraints (22) solvable for the Lagrange multipliers?

These questions will be studied in section 3. Let us assume here, for a moment, that both questions can be answered positively. Then, we obtain a relation $\boldsymbol{\lambda} = \boldsymbol{\lambda}(\mathbf{u})$ from (22) which gives rise to the Maximum Entropy distribution function $\hat{W}(\mathbf{u}, c) = W_{\boldsymbol{\lambda}(\mathbf{u})}(c)$. As outlined before, this particular choice leads to a specific closure relation for the moment system which we call the *Maximum Entropy System*.

1.4.2 Properties of the Maximum Entropy system

Under the assumption that the Maximum Entropy distribution $\hat{W}(\mathbf{u}, c)$ is well defined, we find the following properties.

Proposition:

The Maximum Entropy system is a quasi-linear hyperbolic system of first order, that implies the entropy balance as a concave extension and can thus be brought into the symmetric hyperbolic form.

A detailed investigation can be found in [3], [1] and [13].

1.4.3 The Hermite/Grad system

We study now a further moment system that we call *Hermite/Grad System*. This moment system relies on the **assumption** that a phase density $W(t, x, c)$, which solves the FOKKER PLANCK equation, can be expanded in a series with respect to Hermite functions. We also refer to [8], [15], where the approach has been used for the approximation of the BOLTZMANN equation and the Fokker Planck equation, respectively.

Remark: This assumption confronts us with the problem that the positivity of $W(t, x, c)$ can in general not be guaranteed. This problem does not appear in the *Maximum Entropy system*. However, one can show that at least for $\mathbf{u}$ out of certain open neighborhoods of equilibrium states, the expansion is non-negative.

For the definition of Hermite polynomials and Hermite functions we consider a weighted L^2 space $L^2_\omega(\mathbb{R})$ equipped with the scalar product

$$\left(\Psi, \tilde{\Psi}\right) = \int_{-\infty}^{\infty} \Psi(c)\, \tilde{\Psi}(c)\, \omega(c) dc, \qquad \omega(c) = (W^{eq})^{-1}(c) \tag{23}$$

and corresponding norm $\|\Psi\|^2 = (\Psi, \Psi)$. A complete orthogonal basis in $L^2_\omega(\mathbb{R})$ is given by the Hermite functions Ψ_A which are defined in terms of the Hermite

polynomials H_A:

$$\Psi_A(c) = H_A(c)\, W^{eq}(c), \qquad H_A(c) = (W^{eq})^{-1}(c) \left(-\frac{d}{dc}\right)^A W^{eq}(c). \tag{24}$$

As particular examples, we mention the first six Hermite polynomials

$$\begin{aligned} H_0 &= 1, & H_2 &= c^2 - 1, & H_4 &= c^4 - 6c^2 + 3, \\ H_1 &= c, & H_3 &= c^3 - 3c, & H_5 &= c^5 - 10c^3 + 15c. \end{aligned}$$

Apart from the orthogonality relation

$$(\Psi_A, \Psi_B) = A!\, \delta_{AB}, \tag{25}$$

there are four important identities between Hermite functions Ψ_A of different order and their derivatives Ψ'_A

$$\begin{aligned} \Psi_{A+1} &= -\Psi'_A, & c\Psi'_A + c\Psi_A - A\Psi_{A-1} &= 0, \\ c\Psi_A &= A\Psi_{A-1} + \Psi_{A+1}, & \Psi''_A + A\Psi'_A + A\Psi_A &= 0. \end{aligned} \tag{26}$$

Assuming that the phase density is contained in $L^2_\omega(\mathbb{R})$, we can expand W in terms of Hermite functions

$$W(t,x,c) = \sum_{A=0}^{\infty} \frac{1}{A!} h_A(t,x)\, \Psi_A(c), \quad \text{with} \quad h_A = (W, \Psi_A). \tag{27}$$

The quantities

$$h_A(t,x) = \int_{-\infty}^{\infty} \Psi_A(c)\, W(t,x,c)\, \omega(c) dc = \int_{-\infty}^{\infty} H_A(c)\, W(t,x,c)\, dc \tag{28}$$

are called *Hermite moments*. In analogy to the former case of ordinary moments, we obtain an infinite hierarchy of balance equations for the Hermite moments. The hierarchy can easily be derived from the general equations of balance for the choice $\psi(t,x,c) \in \{H_0(c), H_1(c), H_2(c), ...\}$ and by means of the identities (26). The resulting system reads

$$\frac{\partial h_A}{\partial t} + \frac{\partial (A h_{A-1} + h_{A+1})}{\partial x} = -A h_A. \tag{29}$$

Assuming again that a thermodynamic process is sufficiently described by the first M Hermite moments as variables, we consider

$$\tilde{W}(h_0(t,x), h_1(t,x), ..., h_{M-1}(t,x), c) = \sum_{A=0}^{M-1} \frac{1}{A!} h_A(t,x)\, \Psi_A(c) \tag{30}$$

as a *good* approximation of the exact phase density. This statement will be studied in detail in section 4, where we compare the consequences of (30) with exact analytical solutions of the Fokker Planck equation.

We conclude that the highest Hermite moment h_M, appearing in the highest balance equation, vanishes due to the orthogonality condition (25), and this solves the closure problem. The resulting system of field equations is

$$\frac{\partial h_A}{\partial t} + \sum_{B=0}^{M-1} M_{AB} \frac{\partial h_B}{\partial x} = -\sum_{B=0}^{M-1} R_{AB} h_B, \quad A \in \{0, 1, 2, ...M-1\}, \tag{31}$$

where the constant matrices M_{AB} and R_{AB} are defined by

$$(M_{AB}) = \begin{pmatrix} 0 & 1 & & & & \\ 1 & 0 & 1 & & & \\ & 2 & 0 & 1 & & \\ & & & \cdot & & \\ & & & & \cdot & \\ & & & & M-1 & 0 \end{pmatrix}, \quad (R_{AB}) = \begin{pmatrix} 0 & & & & & \\ & 1 & & & & \\ & & 2 & & & \\ & & & \cdot & & \\ & & & & \cdot & \\ & & & & & M-1 \end{pmatrix}. \tag{32}$$

The system (31) with (32) is called *Hermite/Grad System*. Observe that the *Hermite/Grad System* can be rewritten as a set of equations for ordinary moments by a linear transformation of variables. In the case $M = 5$, which we consider more detailed in section 4, the transformation $\mathbf{u} = Q\mathbf{h}$ is given by

$$Q = \begin{pmatrix} 1 & 0 & 0 & 0 & 0 \\ 0 & 1 & 0 & 0 & 0 \\ 1 & 0 & 1 & 0 & 0 \\ 0 & 3 & 0 & 1 & 0 \\ 3 & 0 & 6 & 0 & 1 \end{pmatrix}. \tag{33}$$

One easily checks that $\mathbf{u} = Q\mathbf{h}$ satisfies the moment system with the closure relation

$$u_5 = -15u_1 + 10u_3. \tag{34}$$

1.4.4 Properties of the Hermite/Grad System

The *Hermite/Grad system* is simpler than the *Maximum Entropy System*, because it is linear. However, it has the hyperbolicity property in common with the *Entropy Maximum System.*

Proposition:

The *Hermite/Grad System* is a linear hyperbolic system of first order, that implies the entropy balance as a concave extension and can thus be brought into the symmetric hyperbolic form.

Proof: The proof relies on the fact, that the matrix M_{AB} has M distinct eigenvalues. Thus its left and right eigenvectors of dimension M exist and can be used to bring the *Hermite/Grad System* into the symmetric form. Moreover, a simple calculation of the entropy density leads to

$$h = -\sum_{A=0}^{M-1} \frac{1}{A!} h_A h_A < 0. \tag{35}$$

We conclude that the entropy density is a concave function of the variables.

2 The initial value problem for the Fokker Planck equation and its exact solution

2.1 The general initial value problem

We consider the Cauchy problem for the linear FOKKER-PLANCK equation in one space dimension

$$\frac{\partial W}{\partial t} + c\,\frac{\partial W}{\partial x} = \frac{\partial}{\partial c}\left(c\,W + \frac{\partial W}{\partial c}\right), \qquad W(0,x,c) = W_0(x,c)\,. \tag{36}$$

To solve this initial value problem, we proceed in three steps: At first, we remove the inhomogeneity of the FOKKER-PLANCK equation by choosing a new phase density $f = f(t,x,c)$, which describes the deviation from equilibrium and is given by

$$W(t,x,c) = W^{eq}(c)\,f(t,x,c)\,, \quad \text{with} \quad W^{eq}(c) = \frac{1}{\sqrt{2\pi}}\,\exp\left(-\frac{c^2}{2}\right). \tag{37}$$

Note that the equilibrium distribution function $W^{eq}(c)$ is a time and space independent solution of the Fokker-Planck equation (1). The resulting equation for f reads

$$\frac{\partial f}{\partial t} + c\,\left(\frac{\partial f}{\partial x} + \frac{\partial f}{\partial c}\right) = \frac{\partial^2 f}{\partial c^2}\,. \tag{38}$$

In the second step we transform the phase space variables x and c by introducing new time dependent variables, viz.

$$\xi = x - c\,\psi(t)\,, \qquad \eta = c\,\psi'(t)\,, \quad \text{with} \quad \psi(t) = 1 - \exp(-t)\,. \tag{39}$$

Note that $t \mapsto (\xi(t,x), \eta(t,x))$ are the characteristic curves of the equation

$$\frac{\partial W}{\partial t} + c\,\frac{\partial W}{\partial x} - c\,\frac{\partial W}{\partial c} = 0 \tag{40}$$

which is (36) up to the term $W + \partial_c^2 W$ on the right hand side.

Rewriting f in terms of ξ and η, we obtain a new quantity $g = g(t, \xi, \eta)$ by

$$f(t, x, c) = g(t, x - c\,\psi(t), c\psi'(t))\,. \tag{41}$$

Obviously we can construct the function g from the function f in a unique way, and vice versa. The phase space function g satisfies the following diffusion equation with time dependent coefficients:

$$\frac{\partial g}{\partial t} = \psi^2\,\frac{\partial^2 g}{\partial \xi^2} - 2\psi\psi'\,\frac{\partial^2 g}{\partial \xi \partial \eta} + \psi'^2\,\frac{\partial^2 g}{\partial \eta^2}\,. \tag{42}$$

In the final step we solve the initial value problem for the diffusion equation (42). To this end we define primitives of the coefficients in the diffusion equation,

$$F(t) = 2\int_0^t \psi(\vartheta)^2\,d\vartheta = 2t - 3 + 4\exp(-t) - \exp(-2t)\,, \tag{43}$$

$$H(t) = 2\int_0^t \psi(\vartheta)\psi'(\vartheta)\,d\vartheta = (1 - \exp(-t))^2\,, \tag{44}$$

$$G(t) = 2\int_0^t \psi'(\vartheta)^2\,d\vartheta = 1 - \exp(-2t)\,, \tag{45}$$

and set for abbreviation

$$\Delta(t) = F(t)G(t) - H(t)^2. \tag{46}$$

The following propositions are then checked by straight forward calculations:

a) We obtain $\Delta(0) = 0$ and $\Delta(t) > 0$ for $t \neq 0$ due to the Cauchy-Schwarz inequality, because the functions ψ and ψ' are not collinear on any time interval.

b) The function $g_* : \mathbb{R}^+ \times \mathbb{R}^2 \to \mathbb{R}$, which is defined by

$$g_*\,(t, \xi, \eta) = \frac{1}{2\pi\sqrt{\Delta\,(t)}}\exp\left[-\frac{G\,(t)\,\xi^2 + 2H\,(t)\,\xi\eta + F\,(t)\,\eta^2}{2\Delta\,(t)}\right], \tag{47}$$

is a solution of the diffusion equation (42) for $t > 0$.

c) g_* satisfies the normalization condition

$$\int_{-\infty}^{+\infty}\int_{-\infty}^{+\infty} g_*(t, \xi, \eta)\,d\xi d\eta = 1\,, \tag{48}$$

which can be proved by the integral substitution

$$u = \frac{G\xi + H\eta}{\sqrt{G\Delta}}\,, \qquad v = \frac{\sqrt{\Delta}\,\eta}{\sqrt{G\Delta}}\,. \tag{49}$$

d) For $t \to 0$ we find the following asymptotic behavior:

$$\begin{aligned} F(t) &= \frac{2}{3}t^3 + O(t^4), & H(t) &= t^2 + O(t^3), \\ G(t) &= 2t + O(t^2), & \Delta(t) &= \frac{1}{3}t^4 + O(t^5). \end{aligned} \tag{50}$$

e) If ξ and η are shifted by the constants ξ', η' then $g_*(t, \xi - \xi', \eta - \eta')$ is also a solution of the diffusion equation (42).

Finally we conclude from a) - e) that g_* is a fundamental solution of (42), i.e. the initial value problem for the diffusion equation (42) with given initial data

$$g(0, \xi, \eta) = g_0(\xi, \eta) \tag{51}$$

is solved by

$$g(t, \xi, \eta) = \int_{-\infty}^{+\infty} \int_{-\infty}^{+\infty} g_0(\xi', \eta')\, g_*(t, \xi - \xi', \eta - \eta')\, d\xi' d\eta' \,. \tag{52}$$

In order to solve the original initial value problem (36) for the FOKKER-PLANCK equation, we conclude from (39) that for $t = 0$ the transformed variables ξ and η meet $\xi = x$ and $\eta = c$. Therefore the initial functions for the problems (38) and (42) are the same, and we calculate $g(0, \xi, \eta) = g_0(\xi, \eta)$ from the given initial function W_0 according to

$$g_0(\xi, \eta) = W_0(\xi, \eta)/W^{eq}(\eta) \,. \tag{53}$$

This is introduced in (52), expressing $g(t, \xi, \eta)$ explicitly by the initial function W_0. The solution of the original initial value problem (36) then reads

$$W(t, x, c) = W^{eq}(c)\, g(t, x - c\,(1 - \exp(-t)), c\, \exp(-t)). \tag{54}$$

To our knowledge, this solution formula has first been presented in [2]. Its current derivation, however, is slightly modified and is better suited to deal with RIEMANN initial value problems.

2.2 The Riemann initial value problem

In order to compare the moment approximations with exact solutions of the FOKKER PLANCK equation, we use simple, physically realizable initial conditions, consisting of two equilibrium states which coexist by some separation mechanism in disjoint space intervals (i.e. RIEMANN initial data). If the separation is removed, the FOKKER PLANCK process evolves with the tendency of levelling out density differences. Relying on the linearity of the FOKKER PLANCK equation, the RIEMANN

problem may serve as a building block for constructing further solutions. Moreover, the RIEMANN solution may serve as an outstanding tool to study the evolution of states which are initially in non-equilibrium. Note that, by reducing the height of the initial density jump to arbitrary small values, the distance from global equilibrium can nevertheless be controlled.

The prescribed initial data of the considered RIEMANN problem are

$$W_0(x,c) = \begin{cases} n_L\, W^{eq}(c) & x \le 0 \\ & \text{for} \\ n_R\, W^{eq}(c) & x > 0 \end{cases} . \tag{55}$$

Here n_L and n_R are given positive constants and $W^{eq}(c)$ is the MAXWELLian phase density (37).

From (55) and (53) we calculate the initial data

$$g_0(\xi,\eta) = \begin{cases} n_L & \xi \le 0 \\ & \text{for} \\ n_R & \xi > 0 \end{cases} \tag{56}$$

which corresponds to the initial value problem of the diffusion equation (42). Recall that $\xi = x$ and $\eta = c$ holds only at $t = 0$. Since the function $g_0(\xi,\eta)$ does not depend on η, it can be read off from (52) that the solution $g(t,\xi,\eta)$ is also independent on η. In this special case the diffusion equation (42) reduces to the simple form

$$\frac{\partial g}{\partial t} = \psi^2 \frac{\partial^2 g}{\partial \xi^2} . \tag{57}$$

Thus in (52) we may avoid the η-integration for the calculation of the solution $g(t,\xi,\eta)$ in the following way: Let us assume that $g(t,\xi,\eta)$ is the η-independent solution of (57) for the RIEMANNian initial data (56). Then we may choose a new function $\hat{g} = \hat{g}(\vartheta,\xi)$ which does not depend on η according to

$$\hat{g}\left(\frac{1}{2}F(t),\xi\right) = g(t,\xi,\eta). \tag{58}$$

The transformation $\vartheta = \frac{1}{2}F(t)$ of the time coordinate in (57) leads us to conclude that $\hat{g}$ solves the simple diffusion equation

$$\frac{\partial \hat{g}}{\partial \vartheta} = \frac{\partial^2 \hat{g}}{\partial \xi^2} . \tag{59}$$

The initial data for $\hat{g}$ are the same as for g and are given by the right hand side of (56). There results the solution

$$\hat{g}(\vartheta,\xi) = n_R\, \Phi(\xi/\sqrt{2\vartheta}) + n_L\, \Phi(-\xi/\sqrt{2\vartheta}), \tag{60}$$

where $\Phi(z)$ denotes the *Error Function*

$$\Phi(z) = \frac{1}{\sqrt{2\pi}} \int_{-\infty}^{z} \exp(-u^2/2)\, du\,. \tag{61}$$

From (54) and (58) we obtain immediately the explicit solution of the FOKKER PLANCK equation (1) for the RIEMANNian initial data (55):

$$W(t,x,c) = W^{eq}(c) \left[n_R\, \Phi\left(\frac{x - c\psi(t)}{\sqrt{F(t)}} \right) + n_L\, \Phi\left(-\frac{x - c\psi(t)}{\sqrt{F(t)}} \right) \right] \tag{62}$$

where $\psi(t) = 1 - \exp(-t)$.

2.3 Ordinary moments calculated from the exact solution

In order to compare solutions of the FOKKER PLANCK equation with those of the moment approximations, we calculate the moments $\mathbf{u} = (u_0, u_1, u_2, u_3, u_4)$ and u_5 from the exact analytical solution (62) of the Riemann problem (36) and (55). First, we rewrite (62) in the form

$$W(t,x,c) = n_R\, W_+(t,x,c) + n_L\, W_-(t,x,c)\,, \tag{63}$$

where the phase densities $W_\pm(t,x,c)$ are given by

$$W_\pm(t,x,c) = W^{eq}(c)\, \Phi\left(\pm \frac{x - c(1 - \exp(-t))}{\sqrt{F(t)}} \right)\,. \tag{64}$$

The *Error Function* obeys the relation $\Phi(z) + \Phi(-z) = 1$ which yields

$$W_+(t,x,c) + W_-(t,x,c) = W^{eq}(c)\,. \tag{65}$$

Next we derive analytical expressions for the moments

$$u_A(t,x) = \int_{-\infty}^{+\infty} c^A\, W(t,x,c)\, dc\,, \quad A \in \{0,1,...,5\} \tag{66}$$

in terms of the moments

$$u_A^\pm(t,x) = \int_{-\infty}^{+\infty} c^A\, W_\pm(t,x,c)\, dc \quad \text{and} \quad u_A^{eq} = \int_{-\infty}^{+\infty} c^A\, W^{eq}(c)\, dc\,. \tag{67}$$

From (65) we obtain at first

$$u_A(t,x) = n_L\, u_A^{eq} + (n_R - n_L)\, u_A^+(t,x)\,. \tag{68}$$

The first contribution $n_L\, u_A^{eq}$ is immediately calculated since

$$\mathbf{u}^{eq} = (1, 0, 1, 0, 3, \ldots)\,. \tag{69}$$

It remains to determine the moments $u_A^+(t,x)$. Since $u_A^+(t,x) \to 0$ for $x \to -\infty$, we may write, with $\psi(t) = 1 - \exp(-t)$,

$$u_A^+(t,x) = \int_{-\infty}^{x} \frac{\partial u_A^+}{\partial x}(t,y)\, dy = \int_{-\infty}^{x} \int_{-\infty}^{+\infty} \bar{c}^A\, W^{eq}(\bar{c})\, \Phi'\left(\frac{y - \bar{c}\psi(t)}{\sqrt{F(t)}}\right) \frac{1}{\sqrt{F(t)}}\, d\bar{c}\, dy. \tag{70}$$

Due to the definition of Φ, the right hand side of (70) can be simplified to

$$u_A^+(t,x) = \frac{1}{\sqrt{F(t)}} \int_{-\infty}^{x} \int_{-\infty}^{+\infty} \bar{c}^A\, W^{eq}(\bar{c})\, W^{eq}\left(\frac{y - \bar{c}\psi(t)}{\sqrt{F(t)}}\right) d\bar{c}\, dy. \tag{71}$$

Using the substitution $(y, \bar{c}) = (z\sqrt{F + \psi^2}, \beta c + \gamma z)$ with

$$\beta(t) = \sqrt{\frac{F\,(t)}{F\,(t) + \psi\,(t)^2}}\,, \qquad \gamma(t) = \frac{\psi\,(t)}{\sqrt{F\,(t) + \psi\,(t)^2}} \tag{72}$$

leads to

$$u_A^+(t,x) = \int_{-\infty}^{\sigma(t,x)} W^{eq}(z) \int_{-\infty}^{+\infty} (\beta c + \gamma z)^A\, W^{eq}(c)\, dc\, dz\,, \tag{73}$$

where σ is defined by

$$\sigma(t,x) = \frac{x}{\sqrt{F\,(t) + \psi\,(t)^2}}. \tag{74}$$

The c-integration of the expressions

$$J_A = J_A(t,z,c) = \int_{-\infty}^{+\infty} (\beta c + \gamma z)^A\, W^{eq}(c)\, dc \tag{75}$$

may easily be done, resulting in

$$\begin{array}{lll} J_0 = 1, & J_2 = \beta^2 + \gamma^2 z^2, & J_4 = 3\beta^4 + 6\beta^2\gamma^2 z^2 + \gamma^3 z^3, \\ J_1 = \gamma z, & J_3 = 3\beta^2\gamma z + \gamma^3 z^3\,. & \end{array} \tag{76}$$

Finally, the calculation of the z-integrals in (71) relies on the recurrence relations

$$\Phi_0(\sigma) = \Phi(\sigma)\,,\ \Phi_1(\sigma) = -W^{eq}(\sigma)\,,\ \Phi_{n+2}(\sigma) = (n+1)\,\Phi_n(\sigma) - \sigma^{n+1}\, W^{eq}(\sigma) \tag{77}$$

for the *Momentum Error Function*s

$$\Phi_A(\sigma) = \int_{-\infty}^{\sigma} z^A\, W^{eq}(z)\, dz\,. \tag{78}$$

If we use these relations and equations (68), (73) we obtain

$$\begin{aligned}
u_0 &= n_L + (n_R - n_L)\,\Phi(\sigma)\,, && (79)\\
u_1 &= -(n_R - n_L)\,\gamma\,W^{eq}(\sigma)\,, && (80)\\
u_2 &= n_L + (n_R - n_L)\,(\Phi(\sigma) - \gamma^2\sigma\,W^{eq}(\sigma))\,, && (81)\\
u_3 &= -(n_R - n_L)\,\gamma\,(\gamma^2\sigma^2 - \gamma^2 + 3)\,W^{eq}(\sigma)\,, && (82)\\
u_4 &= 3n_L + (n_R - n_L)\,(3\Phi(\sigma) - \gamma^2\sigma(\gamma^2\sigma^2 - 3\gamma^2 + 6)W^{eq}(\sigma))\,, && (83)\\
u_5 &= -(n_R - n_L)\,\gamma\,(\gamma^4\sigma^4 + (10\gamma^2 - 6\gamma^4)\sigma^2 - 10\gamma^2 + 15 + 3\gamma^4)\,W^{eq}(\sigma)\,. && (84)
\end{aligned}$$

where

$$\gamma(t) = \frac{1-\exp(-t)}{\sqrt{2(\exp(-t)-1+t)}}, \qquad \sigma(t,x) = \frac{x}{\sqrt{2(\exp(-t)-1+t)}}\,. \tag{85}$$

2.4 Normalized moments

In order to visualize the moments $\mathbf{u} = (u_0, \ldots, u_4)$ of the phase density W, we will resort to the following normalization: at first we define three functions of $\mathbf{u}$

$$n = u_0, \qquad v = u_1/n, \qquad \theta = u_2/n - v^2 \tag{86}$$

which represent the number density n of the BROWNian particles, their average velocity v, and the kinetic energy $n\theta/2$ of their random movement.

Next, we define normalized moments of the phase density W by

$$\hat{u}_A(t,x) := \int_{-\infty}^{\infty} \frac{1}{n(t,x)} \left(\frac{c - v(t,x)}{\sqrt{\theta(t,x)}}\right)^A W(t,x,c)dc. \tag{87}$$

A straight forward calculation reveals a relation between the ordinary moments $\mathbf{u}$ and $\hat{\mathbf{u}}$ of the form

$$\hat{\boldsymbol{u}} = \frac{1}{n} L\left(-\frac{v}{\sqrt{\theta}}\right) D\left(\frac{1}{\theta}\right) \boldsymbol{u}, \qquad \boldsymbol{u} = nD(\theta)L\left(\frac{v}{\sqrt{\theta}}\right)\hat{\boldsymbol{u}} \tag{88}$$

where

$$L(\alpha) = \begin{pmatrix} 1 & & & & \\ \alpha & 1 & & & \\ \alpha^2 & 2\alpha & 1 & & \\ \alpha^3 & 3\alpha^2 & 3\alpha & 1 & \\ \alpha^4 & 4\alpha^3 & 6\alpha^2 & 4\alpha & 1 \end{pmatrix}, \qquad D(\alpha) = \begin{pmatrix} 1 & & & & \\ & \alpha^{\frac{1}{2}} & & & \\ & & \alpha & & \\ & & & \alpha^{\frac{3}{2}} & \\ & & & & \alpha^2 \end{pmatrix}. \tag{89}$$

By construction, we always have $\hat{u}_1 = 1, \hat{u}_2 = 0, \hat{u}_3 = 1$. Taking into account that the normalized moments of any equilibrium distribution are of the form $\hat{\mathbf{u}}^{eq} = (1, 0, 1, 0, 3)$, it is natural to introduce the functions

$$q(\mathbf{u}) = \hat{u}_3, \qquad s(\mathbf{u}) = \hat{u}_4 - 3 \tag{90}$$

which measure the deviation from equilibrium. Then, using the considerations above, we can represent any moment vector $\mathbf{u} = (u_0, \ldots, u_4)$ in a one-to-one fashion by specifying the five quantities n, v, θ, q, s.

2.5 Structure of the exact solution

First, we consider the moments of the FOKKER PLANCK solution for a jump from $n_L = 1$ to $n_R = 1/2$ at times $t = 0.25$ (solid lines), $t = 0.75$ (dashed lines) and $t = 1.5$ (dotted lines). The number density n and the average velocity v of the BROWNian particles are given in Fig. 1 and 2.

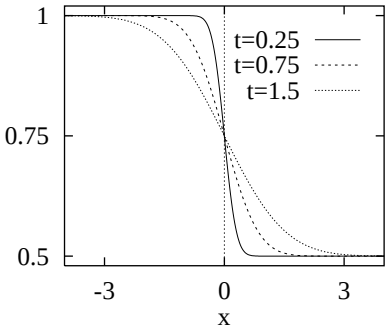

Figure 1: Number density n

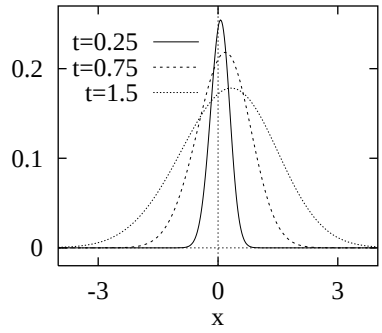

Figure 2: Average velocity v

The moments θ, q and s are shown in Fig. 3, 4 and 5 respectively.

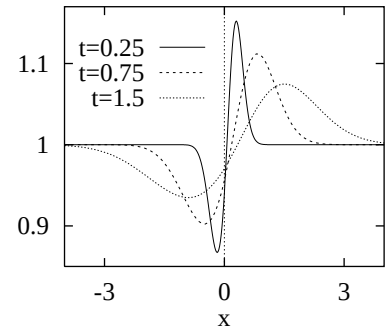

Figure 3: Moment θ

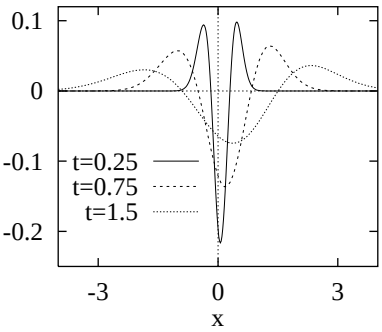

Figure 4: Moment q

Another representation of the solution is obtained in the (q, s)-diagram. We calculate $q(t, x) = q(\mathbf{u}(t, x))$ and $s(t, x) = s(\mathbf{u}(t, x))$ for $t = 0.75$, and $x \in \mathbb{R}$ as specified in the previous section.

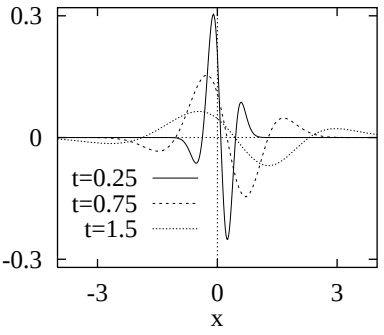

Figure 5: Moment s

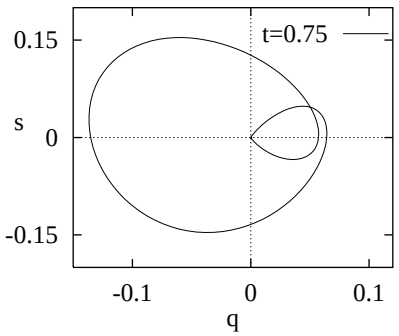

Figure 6: Solution in (q, s) diagram

Since at $x = \pm\infty$, the solution is in equilibrium, the curve $x \mapsto (q(t,x), s(t,x))$ starts and ends in the normalized equilibrium point $(0,0)$ (see Fig. 6). For increasing x, starting at $x = -\infty$, the (q,s) curve goes down into the fourth quadrant $\{q < 0,\ s > 0\}$, then into the upper half plane $\{s > 0\}$ where it crosses the line $q = 0$. After coming back into the lower half plane, it crosses $s = 0$ again and approaches, for $x \to +\infty$, the equilibrium point within the first quadrant.

For a stronger jump from $n_L = 1$ to $n_R = 0.01$ also at $t = 0.75$, the corresponding (q,s) diagram is shown in Fig. 7.

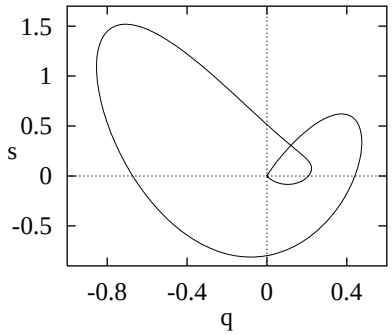

Figure 7: Solution for strong density jump

Again, the curves are traversed counter-clock-wise but the maximal distance from equilibrium has much increased.

Let us now turn to the case of small jumps $n_L = 1$, $n_R = 1 - \varepsilon$ where we are particularly interested in the asymptotic behavior of the initial value problems for small values $\varepsilon \ll 1$. If we consider only contributions that are of linear order in ε, we obtain from relations (79) to (83) and the definition of q and s

$$q = \varepsilon\gamma^3(\sigma^2 - 1)\, W^{eq}(\sigma) \,+\, O(\varepsilon^2)\,, \tag{91}$$

$$s = \varepsilon\gamma^4\sigma\,(\sigma^2 - 3)\, W^{eq}(\sigma) \,+\, O(\varepsilon^2)\,. \tag{92}$$

In a numerical study, we compare the curve $x \mapsto (q(t_0,x), s(t_0,x))/\varepsilon$ based on the exact normalized moments with their asymptotic representations for $t_0 = 0.01$ and

different values of $\varepsilon = n_R - n_L$, namely for $\varepsilon = 0.5$, $\varepsilon = 0.25$, $\varepsilon = 0.05$. In Fig. 8, the solid line represents the asymptotic curve which is approached by the exact Fokker-Planck curves for larger ε (in decreasing order: long dashes, short dashes, dotted). For $\varepsilon \leq 0.01$, the scaled curves basically fall on top of the asymptotic one.

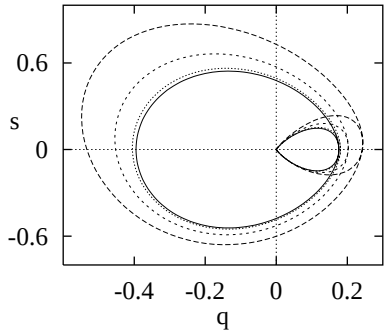

Figure 8: Scaled solutions for different density jumps

Another important observation is that, for small times $t > 0$, the moments depend essentially on x/t only. In fact, since $\psi(t) = 1 - \exp(-t) = t + O(t^2)$ we find from (72), (74) and (50) that

$$\gamma(t) = 1 + O(t^1), \qquad \sigma(t,x) = x/t + O(t^1). \tag{93}$$

Now we may read off from (79)-(84) that a variation in t will not affect the form of the curve $x \mapsto (q(t,x), s(t,x))$, as long as t is small enough.

3 Some properties of the Maximum Entropy system

As we have seen in section 1.4.1, the essential feature which distinguishes the *Maximum Entropy system* for $\mathbf{u} = (u_0, \ldots, u_{M-1})$ from other moment systems is the closure relation $u_M = F(\mathbf{u})$. It is obtained by taking the ordinary velocity moment

$$F(\mathbf{u}) = \int_{-\infty}^{+\infty} c^M W_{\boldsymbol{\lambda}}(\mathbf{u}, c)\, dc \tag{94}$$

of the Maximum Entropy distribution $W_{\boldsymbol{\lambda}}(\mathbf{u}, c)$ which solves the constrained optimization problem already introduced in (17)

$$\max\{H(W) : W \in \mathcal{W}_M,\ \boldsymbol{\mu}^{(M)}(W) = \boldsymbol{u}\}. \tag{95}$$

In particular, F is only defined for those $\mathbf{u} \in U_M \subset \mathbb{R}^M$ for which (95) has a unique solution. In the following, we are going to investigate this set U_M which makes up the domain of definition of the *Maximum Entropy system*.

3.1 Solving the Maximum Entropy problem

In section 1.4.1 we have derived the solution of (95) in the form

$$W_{\boldsymbol{\lambda}}(c) = W^{eq}(c) \exp\left(\sum_{A=0}^{M-1} \lambda_A c^A - 1\right) \tag{96}$$

where $\boldsymbol{\lambda}$ is determined from

$$u_A = \int_{-\infty}^{\infty} c^A W_{\boldsymbol{\lambda}} dc, \quad A \in \{0, 1, ..., M-1\} \tag{97}$$

Although these considerations have only been formal, a more detailed investigation shows that the result is nevertheless correct. More precisely, whenever (97) is solvable for $\boldsymbol{\lambda}$, then (96) is the unique solution of the Maximum Entropy problem and vice versa (see [9, 11]).

Before we use this result, let us remark that in all our considerations $\boldsymbol{u}$ should be the moment vector of some $W \in \mathcal{W}_M$ (otherwise, the maximum in (95) is taken over the empty set). Note that $\mathcal{W}_M$ is a convex cone (because of the condition $W \geq 0$) so that the same holds for $K_M = \boldsymbol{\mu}^{(M)}(\mathcal{W}_M)$, which is an open subset of $\mathbb{R}^M$, see [11]. Another important observation is that $W_{\boldsymbol{\lambda}}$ is contained in $\mathcal{W}_M$ only for $\boldsymbol{\lambda}$ from a certain subset $\Lambda_M \subset \mathbb{R}^M$.

In the case $M = 1$, we find in particular $\Lambda_1 = \mathbb{R}$ and $K_1 = (0, \infty)$. Since any $u_0 > 0$ can be written as c-integral of

$$W_{\boldsymbol{\lambda}}(c) = W^{eq}(c) \exp(\lambda_0 - 1), \qquad \lambda_0 = 1 + \log u_0 \tag{98}$$

we conclude that (95) is solvable for any $\boldsymbol{u} \in K_1$. Similarly, for $M = 2$ we find $\Lambda_2 = \mathbb{R}^2$, $K_2 = \{(u_0, u_1)^T : u_0 > 0, u_1 \in \mathbb{R}\}$ and any $\boldsymbol{u} \in K_2$ can be written as moment vector of

$$W_{\boldsymbol{\lambda}}(c) = W^{eq}(c) \exp(\lambda_0 + \lambda_1 c - 1), \qquad \lambda_1 = u_1/u_0, \quad \lambda_0 = 1 + \log u_0 - \lambda_1^2/2. \tag{99}$$

The next case, $M = 3$ is characterized by $\Lambda_3 = \{\boldsymbol{\lambda} \in \mathbb{R}^3 : \lambda_2 < 1/2\}$ and

$$K_3 = \{(u_0 = n, u_1 = nv, u_2 = n(\theta + v^2) : n > 0,\, v \in \mathbb{R},\, \theta > 0\}. \tag{100}$$

Any element of K_3 can be obtained as moment vector of the MAXWELLian

$$W(c) = \frac{n}{\sqrt{2\pi\theta}} \exp\left(-\frac{(c-v)^2}{2\theta}\right) \tag{101}$$

which can obviously be written as $W_{\boldsymbol{\lambda}}$ with a suitable $\boldsymbol{\lambda} \in \Lambda_3$. For $M > 3$, integrability of $W_{\boldsymbol{\lambda}}$ leads to conditions like $\lambda_M < 0$ if M is odd and $\lambda_M = 0$, $\lambda_{M-1} < 0$ if M is even. Identifying $\Lambda_M \subset \mathbb{R}^M$ with $\Lambda_M \times \{0\} \subset \mathbb{R}^{M+1}$, we find that $\Lambda_M = \Lambda_{M-1}$ if $M > 3$ is even and $\Lambda_M = \{\boldsymbol{\lambda} \in \mathbb{R}^M : \lambda_{M-1} < 0\} \cup \Lambda_{M-2}$ for $M > 3$ being odd.

Lemma 1 *Let $M \in \mathbb{N}$ and $\boldsymbol{u} \in \mathbb{R}^M$. Then, the Maximum Entropy problem* (95) *is uniquely solvable if and only if $\boldsymbol{u} \in U_M$ which is given by $U_M = \boldsymbol{\mu}^{(M)}(\Lambda_M)$.*

Proof: The cases $M \leq 3$ have already been treated above. For $M > 3$, the proof can be found in [11], section 7. Note that in this reference, the considerations are based on the entropy $H^*(W) = -\int\limits_{-\infty}^{\infty} W \log W dc$. However, in the case $M > 3$, the results can be used because (95) is equivalent to the Maximum Entropy problem based on H^*. Indeed, we have

$$H(W) = -\int\limits_{-\infty}^{\infty} W \log W dc + \int\limits_{-\infty}^{\infty} W \log W^{eq} dc = H^*(W) - \frac{1}{2}(\log(2\pi)u_0 + u_2), \quad (102)$$

where u_0 and u_2 are prescribed in the case $M \geq 3$. ■

The result of Lemma 1 implies that for even $M > 3$, the set of admissible moments are essentially those of the case $M - 1$ since $\Lambda_M = \Lambda_{M-1}$. In particular, U_M is a hyper-plane in K_M so that a generic moment vector $\boldsymbol{u} \in K_M$ will not be contained in U_M. Let us therefore concentrate on the case $M = 2N + 1$ with $N > 1$.

Theorem 2 *Let $M = 2N + 1$ for some $N > 1$ and assume that $\boldsymbol{u} \in K_M$. Then, the constrained optimization problem* (95) *has no solution if $\boldsymbol{u} \in E_M$ with*

$$E_M = \{\boldsymbol{u} \in \mathbb{R}^M : \boldsymbol{u} = \boldsymbol{\mu}^{(M)}(W_{\boldsymbol{\lambda}^*}) + \alpha \boldsymbol{e}_M,\, \alpha > 0,\, \boldsymbol{\lambda}^* \in \Lambda_{M-2}\}, \quad (103)$$

where $\boldsymbol{e}_M$ is the M-th unit vector. In other words, $U_M = K_M \backslash E_M$.

Proof: We will show only one part of the statement which implies $E_M \subset U_M^c$. For the full argument, we again refer to [11].

Our proof uses strict convexity of the function $Z : \Lambda_M \mapsto \mathbb{R}$ defined by

$$Z(\boldsymbol{\lambda}) = \int\limits_{-\infty}^{\infty} W_{\boldsymbol{\lambda}} dc - \sum_{A=0}^{M-1} \lambda_A u_A \quad (104)$$

which follows from the positive definiteness of the matrix of second derivatives

$$\frac{\partial^2 Z(\boldsymbol{\lambda})}{\partial \lambda_A \partial \lambda_B} = \int\limits_{-\infty}^{\infty} c^A c^B W_{\boldsymbol{\lambda}} dc. \quad (105)$$

Indeed, taking any vector $0 \neq \boldsymbol{a} \in \mathbb{R}^M$, we find

$$\sum_{A,B=0}^{M-1} \frac{\partial^2 Z(\boldsymbol{\lambda})}{\partial \lambda_A \partial \lambda_B} a_A a_B = \int\limits_{-\infty}^{\infty} \left(\sum_{A=0}^{M-1} a_A c^A \right)^2 W_{\boldsymbol{\lambda}} dc > 0 \quad (106)$$

since $W_{\boldsymbol{\lambda}}$ is strictly positive and the square of a non-zero polynomial is positive up to at most finitely many points.

Let now $\boldsymbol{u} = \boldsymbol{\mu}^{(M)}(W_{\boldsymbol{\lambda}^*}) + \alpha \boldsymbol{e}_M$ be contained in E_M. In a contradiction argument, we assume that there exists $\bar{\boldsymbol{\lambda}} \in \Lambda_M$ with $\boldsymbol{u} = \boldsymbol{\mu}^{(M)}(W_{\bar{\boldsymbol{\lambda}}})$. Since

$$\nabla Z(\boldsymbol{\lambda}) = \boldsymbol{\mu}^{(M)}(W_{\boldsymbol{\lambda}}) - \boldsymbol{u}, \tag{107}$$

the gradient vanishes at $\boldsymbol{\lambda} = \bar{\boldsymbol{\lambda}}$ which therefore is the unique minimum of the strictly convex function Z. If we consider Z on the line segment from $\boldsymbol{\lambda}^*$ to $\bar{\boldsymbol{\lambda}}$, i.e.

$$g(s) := Z(\boldsymbol{\lambda}^* + s(\bar{\boldsymbol{\lambda}} - \boldsymbol{\lambda}^*), \qquad s \in [0,1] \tag{108}$$

we immediately conclude that g is also strictly convex and has a minimum at $s = 1$. In particular, $g'(0) < 0$ which implies

$$0 > g'(0) = (\bar{\boldsymbol{\lambda}} - \boldsymbol{\lambda}^*) \cdot \nabla Z(\boldsymbol{\lambda}^*). \tag{109}$$

According to (107), the gradient is the difference between $\boldsymbol{u}^* = \boldsymbol{\mu}^{(M)}(f_{\boldsymbol{\lambda}^*})$ and $\boldsymbol{u}$ so that

$$0 > g'(0) = (\bar{\lambda}_{M-1} - \lambda^*_{M-1})(u^*_{M-1} - \bar{u}_{M-1}) = -\alpha(\bar{\lambda}_{M-1} - \lambda^*_{M-1}). \tag{110}$$

Since $\alpha > 0$ and $\lambda^*_{M-1} = 0$, we conclude $\bar{\lambda}_{M-1} > 0$ in contradiction to the assumption $\bar{\lambda} \in \Lambda_M$. ∎

We remark that the proof of Theorem 2 relies on the fact that $W_{\boldsymbol{\lambda}}$ is not integrable for $\lambda_{M-1} > 0$. In cases where the underlying velocity space is bounded, however, this argument does not apply and one can show that the Maximum Entropy problem is always solvable in this case. Also, for other entropy functionals, the Maximum Entropy distribution $W_{\boldsymbol{\lambda}}$ has a different form and thus other integrability conditions apply.

3.2 The domain of definition of the Maximum Entropy system

Since we are particularly interested in the case of *Maximum Entropy Systems* with more than three moments, we restrict ourselves to the case $M = 2N+1$ with $N > 1$. According to Theorem 2, we see that the domain of definition U_M of the system is given by $U_M = K_M \backslash E_M$. While K_M has a simple geometry (an open, convex cone), the set E_M is much more complicated. Recalling that

$$E_M = \{\boldsymbol{u} \in \mathbb{R}^M : \boldsymbol{u} = \boldsymbol{\mu}^{(M)}(W_{\boldsymbol{\lambda}^*}) + \alpha \boldsymbol{e}_M,\ \alpha > 0,\ \boldsymbol{\lambda}^* \in \Lambda_{M-2}\}. \tag{111}$$

we conclude that E_M is an $(M-1)$–dimensional manifold in $\mathbb{R}^M$ which is obtained by attaching half-lines to every point of the $(M-2)$–dimensional manifold consisting of $\boldsymbol{\mu}^{(M)}(\Lambda_{M-2})$. Using the following proposition, we find that U_M is *not* convex.

Proposition 3 *Let $C \subset \mathbb{R}^M$ be open, convex, and non-empty. Let further $\emptyset \neq A \subset \mathbb{R}^M$ with $\mathrm{int}(A) = \emptyset$ and $A \cap C \neq \emptyset$. Then, $C \backslash A$ is not convex.*

Proof: The proof is elementary and uses the fact that in a neighborhood of $\boldsymbol{x} \in A \cap C$ one can find points from the set $C \backslash A$ such that $\boldsymbol{x}$ is in their convex hull. ■

A second important observation is that the equilibrium states $\boldsymbol{u}^{eq} = \boldsymbol{\mu}^{(M)}(e^{\gamma W^{eq}})$ are always located on the boundary of U_M. This follows immediately from the definition of E_M because $\gamma \boldsymbol{e}_1 \in \Lambda_{M-2}$. Since the production terms P_A on the right hand side of the moment system (14) have the tendency to bring the system closer to equilibrium, the solution will naturally be close to the boundary of the domain of definition of the system. In fact, for the most simple setup, the initial value $\boldsymbol{u}^0$ will consist of piecewise constant equilibrium states so that $\boldsymbol{u}^0(\mathbb{R}) \subset \partial U_M$. In this very natural situation, little can be said about solvability of the system. Even for smooth solutions, the usual existence result for symmetric hyperbolic problems does not apply since it is based on the assumption that the range of the initial value $\boldsymbol{u}^0(\mathbb{R})$ is contained in a compact set of the *interior* of the domain of definition [14].

In conclusion, we can say that, although being symmetric hyperbolic, the *Maximum Entropy system*s for $M > 3$ lack two desirable properties: first, the domain of definition is not convex and second, the equilibrium points (i.e. the solutions of $P_A(\boldsymbol{u}) = 0$, $A = 0, \ldots, M-1$) are not located in the interior of U_M.

3.3 The special case of five moments

To illustrate the results of the previous sections, we choose the case $M = 5$. In this particular situation, it is possible to visualize the geometry of the domain of definition U_5 by considering the intersection with the affine plane

$$P = \{\boldsymbol{u} \in \mathbb{R}^5 : \boldsymbol{u} = (1, 0, 1, q, 3+s)^T,\ q, s \in \mathbb{R}\} \tag{112}$$

In [10] it is shown that the intersection $P \cap K_5$ is given by

$$\hat{K}_5 = \{(1, 0, 1, q, 3+s)^T : q \in \mathbb{R},\ s > q^2 - 2\}. \tag{113}$$

The point $(q, s) = (0, 0)$ is the only equilibrium point in $\hat{K}_5$. Intersecting the four–dimensional manifold E_5 of inadmissible moments with the plane P, we find the half line $P \cap E_5 = \hat{E}_5 = \{(1, 0, 1, 0, 3+s)^T : s > 0\}$ which emanates at the equilibrium point. In Fig. 9 which shows $\hat{U}_5 = \hat{K}_5 \backslash \hat{E}_5 = U_5 \cap P$, it is clearly visible that U_5 is not convex because of the inner boundary $\hat{E}_5$.

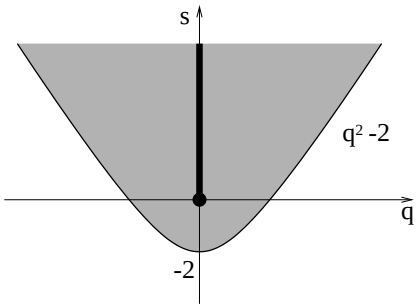

Figure 9: Cut through domain of definition of the Maximum Entropy system

It is important to note that the set $\hat{U}_5$ contains all essential features of U_5. Mathematically, this property manifests itself in a bijection between U_5 and the product of the simple cone K_3 and $\hat{U}_5$. Indeed, as we have seen in section 2, any $\boldsymbol{u} \in U_5$ is uniquely characterized by its first three moments (u_0, u_1, u_2) and the normalized moments $\hat{\mathbf{u}} \in \hat{U}_5$. Suppressing the information about the first three moments u_0, u_1, u_2, we can thus visualize a general moment vector by the two quantities $q(\boldsymbol{u}) = \hat{u}_3$ and $s(\boldsymbol{u}) = \hat{u}_4 - 3$ in the (q, s)-plane P. Since the normalization maps the set of inadmissible vectors E_5 bijectively onto the half–line $\hat{E}_5$, we can easily decide based on $q(\boldsymbol{u})$ and $s(\boldsymbol{u})$ whether $\boldsymbol{u} \in U_5$. More precisely, if $q(\boldsymbol{u}) = 0$ and $s(\boldsymbol{u}) > 0$, the vector $\boldsymbol{u}$ is not in U_5.

Conversely, it is enough to know the flux function for the moments $\hat{\boldsymbol{u}}(q, s) = (1, 0, 1, q, 3 + s)^T \in \hat{U}_5$ because any vector $\boldsymbol{u} \in U_5$ can be composed of some $\hat{\boldsymbol{u}}(q, s)$ and $(u_0, u_1, u_2) \in K_3$ and the relation between $F(\boldsymbol{u})$ and $F(\hat{\boldsymbol{u}}(q, s))$ is known explicitly

$$F(\mathbf{u}) = n \left(\theta^{\frac{5}{2}} F(\hat{\mathbf{u}}) + 5\theta^2 (s + 3)v + 10\theta^{\frac{3}{2}} q v^2 + 10\theta v^3 + v^5 \right). \tag{114}$$

Let us apply this observation to the investigation of the flux function $u_5(\mathbf{u}) = F(\mathbf{u})$ of the *Maximum Entropy system* at the inner boundary $\hat{E}_5$.

Proposition 4 *Let $\hat{\boldsymbol{u}}(q, s) = (1, 0, 1, q, 3 + s)^T \in \hat{U}_5$. We then have the estimate $qF(\hat{\boldsymbol{u}}(q, s)) \geq 2s$.*

The proof of this important proposition is found in [10]. Investigating $F(\hat{\boldsymbol{u}}(q, s))$ for some fixed $s > 0$ and $|q| \to 0$, we see that F is singular at $\hat{E}_5$ and with

$$|F(\hat{\boldsymbol{u}}(q, |q|^{1-\alpha}))| \geq 2|q|^{-\alpha}, \qquad \alpha > 0 \tag{115}$$

it even follows that the flux is singular in the equilibrium point $\hat{\boldsymbol{u}}(0, 0)$.

3.4 A Formal Linearization of the Maximum Entropy system

Since the evaluation of the flux function F in the *Maximum Entropy system* is complicated it is natural to think of a linearization especially since solutions are

typically close to an equilibrium state. As we have seen, however, a linearization in equilibrium points is an "analytical crime" for two reasons: firstly, equilibrium points are located on the boundary of the domain of definition and secondly, the flux is singular at these points. The reason why this approach is nevertheless pursued is also twofold: since the flux function is not explicitly given, the singularity is not directly visible and, as we will see in the following, the Taylor expansion is formally possible, despite the singular behavior.

In order to derive the "linearized" system, we have to expand $u_5(\mathbf{u}) = F(\mathbf{u})$ which is the only non-linear term in the equation. Since the equilibrium distributions are of the form $W_{\boldsymbol{\lambda}^{eq}} = nW^{eq}$ with $n > 0$ (i.e. $\boldsymbol{\lambda}^{eq} = (1 + \log n)\boldsymbol{e}_1$), the moments at which we want to expand are of the form $\boldsymbol{u}^{eq} = n\boldsymbol{\mu}^{(M)}(W^{eq})$. To avoid expansion in the singular point $\boldsymbol{u}^{eq}$ itself, we first slightly perturb the state to $\boldsymbol{u}_\varepsilon^{eq} \in \mathrm{int}(U_M)$. Then, we can use that the mapping $\boldsymbol{u} \mapsto \boldsymbol{\lambda} = \boldsymbol{\lambda}(\boldsymbol{u})$ is infinitely smooth and invertible on $\mathrm{int}(U_M)$ (see [11]). A linearization of $F(\boldsymbol{u}) = \int_{-\infty}^{\infty} c^M W_{\boldsymbol{\lambda}(\boldsymbol{u})} dc$ is obtained by linearizing $W_{\boldsymbol{\lambda}(\boldsymbol{u})}$ around $\boldsymbol{u}_\varepsilon^{eq}$. Afterwards, we go to the limit $\boldsymbol{u}_\varepsilon^{eq} \to \boldsymbol{u}^{eq}$ in such a way that all terms in the expansion remain bounded. In the case of five moments, the way in which $\boldsymbol{u}^{eq}$ has to be approached can be visualized in the (q, s) plane. By choosing the s-component always negative, for example, the vector $\hat{\boldsymbol{u}}_\varepsilon^{eq}$ never enters the region where Proposition 4 predicts a singular behavior.

We thus have

$$W_{lin}^{\varepsilon}(\boldsymbol{u}; c) = W_{\boldsymbol{\lambda}_\varepsilon^{eq}} + \sum_{A,B=0}^{M-1} \frac{\partial W_{\boldsymbol{\lambda}_\varepsilon^{eq}}}{\partial \lambda_A} \left.\frac{\partial \lambda_A}{\partial u_B}\right|_{\boldsymbol{u}_\varepsilon^{eq}} (u_B - u_{\varepsilon B}^{eq}). \tag{116}$$

Using that $\frac{\partial W_{\boldsymbol{\lambda}}}{\partial \lambda_A} = c^A W_{\boldsymbol{\lambda}}$ and the fact that $\left(\frac{\partial \lambda_A}{\partial u_B}\right)_{AB}$ is the inverse of the matrix

$$\left(\frac{\partial u_A}{\partial \lambda_B}\right)_{AB} \qquad \text{with} \qquad \frac{\partial u_A}{\partial \lambda_B} = \int_{-\infty}^{\infty} c^A c^B W_{\boldsymbol{\lambda}} dc, \tag{117}$$

we get

$$W_{lin}^{\varepsilon}(\boldsymbol{u}; c) = \left(1 + \sum_{A,B=0}^{M-1} c^A \left(\left.\frac{\partial \boldsymbol{u}}{\partial \boldsymbol{\lambda}}\right|_{\boldsymbol{\lambda}_\varepsilon^{eq}}\right)_{AB}^{-1} (u_B - u_{\varepsilon B}^{eq})\right) W_{\boldsymbol{\lambda}_\varepsilon^{eq}}. \tag{118}$$

Letting now ε tend to zero, we obtain

$$W_{lin}(\boldsymbol{u}; c) = \left(1 + \sum_{A,B=0}^{M-1} c^A S_{AB} (u_B - u_B^{eq})\right) nW^{eq} \tag{119}$$

where (S_{AB}) is the inverse of the positive definite matrix $\int_{-\infty}^{\infty} c^A c^B nW^{eq} dc$ which can

be calculated explicitly. Finally, we obtain the linearized flux function

$$F^{lin}(\boldsymbol{u}) = \int_{-\infty}^{\infty} c^M W_{lin}(\boldsymbol{u}; c) dc =$$
$$= n \left(\int_{-\infty}^{\infty} c^M W^{eq}\, dc + \sum_{A,B=0}^{M-1} a_{AB}(u_B - u_B^{eq}) \int_{-\infty}^{\infty} c^{M+A} W^{eq}\, dc \right).$$

In the particular case of five moments, the matrix (S_{AB}) is given by

$$(S_{AB}) = \frac{1}{n} \begin{pmatrix} \frac{15}{8} & 0 & -\frac{5}{4} & 0 & \frac{1}{8} \\ 0 & \frac{5}{2} & 0 & -\frac{1}{2} & 0 \\ -\frac{5}{4} & 0 & 2 & 0 & -\frac{1}{4} \\ 0 & -\frac{1}{2} & 0 & \frac{1}{6} & 0 \\ \frac{1}{8} & 0 & -\frac{1}{4} & 0 & \frac{1}{24} \end{pmatrix} \tag{120}$$

so that the linearized flux function is

$$F^{lin}(\boldsymbol{u}) = -15u_1 + 10u_3. \tag{121}$$

Note that this expression is identical to (34) obtained in the HERMITE/GRAD approach. The same observation is, in fact, true for the case of general M.

4 Comparison of moment approximations

In order to compare the five moment Maximum Entropy approach and GRAD's method with the exact solution of the FOKKER PLANCK equation, we use the RIEMANN problem discussed in section 2. We remark that for small jumps in the initial density, the distance of the solution from global equilibrium can be controlled. In the framework of the moment methods, this implies that even with only five moments, one should get satisfactory approximations if the jump is sufficiently small.

Unfortunately, the natural idea to solve all problems for the same initial values in order to compare the results, does not work. The reason is that the initial moment vectors

$$\mathbf{u}^0(x) = \begin{cases} n_L \mathbf{u}^{eq} & x \le 0 \\ n_R \mathbf{u}^{eq} & x > 0 \end{cases} \qquad \mathbf{u}^{eq} = (1, 0, 1, 0, 3) \tag{122}$$

are located exactly on the boundary ∂U_5 of the domain of definition of the *Maximum Entropy System*. Thus, for the *Maximum Entropy System*, it is not clear whether there exists a solution at all. Practical problems in numerical approximations are related to the singularity of the flux in equilibrium points. Since the transport of information can be infinitely fast, the use of explicit schemes is ruled out because

the CFL condition enforces arbitrarily small time steps. An implicit method, on the other hand, requires the solution of non-linear equations involving the singular flux function, where solvability is again a problem.

In view of these difficulties, which already indicate a severe drawback of the *Maximum Entropy system*, we resort to some indirect argument: given the solution of the FOKKER PLANCK equation for some RIEMANN initial value with small jump, we assume that the solutions of the HERMITE/GRAD equations and the *Maximum Entropy system* exist and are close to the FOKKER PLANCK solution. This is the basic idea of all moment methods. Hence, if we plug the FOKKER PLANCK solution into the moment systems, we expect a reasonably small residue. Since, by construction, the first four equations in both systems are satisfied exactly by the FOKKER PLANCK solution $\mathbf{u}$, a residue appears only in the last equation and has the form $\partial_x(F^{lin}(\mathbf{u}) - u_5)$ for the HERMITE/GRAD system and $\partial_x(F(\mathbf{u}) - u_5)$ for the *Maximum Entropy system*. Since $\mathbf{u}$ and u_5 are explicitly given in (79) to (84), the residues can easily be calculated. In addition, we also compare the distribution functions following from the three approaches.

4.1 The residues

In section 2, we have seen that for small density jumps $n_L = 1$, $n_R = 1 - \varepsilon$ in the initial density and small times $t > 0$, the curve $x \mapsto (q_\varepsilon(t,x), s_\varepsilon(t,x))/\varepsilon$ built from the FOKKER PLANCK solution $\mathbf{u}_\varepsilon$ is essentially independent of t and ε. Consequently, the same holds for the quotient $s_\varepsilon/q_\varepsilon$ which, in view of Proposition 4, yields an estimate for the non-linear flux function F in the *Maximum Entropy system*. In Fig. 10, a plot is given which shows the lower bound for $|F(\mathbf{u}_\varepsilon(t,x))|$. The actual values of $F(\mathbf{u}_\varepsilon(t,x))$ together with $F^{lin}(\mathbf{u}_\varepsilon(t,x))$ and $u_{\varepsilon,5}(t,x)$ are presented in Fig. 11. In all our calculations we have chosen $\varepsilon = 0.01$ and $t = 0.01$, but as noted above, this particular choice does not influence the behavior decisively.

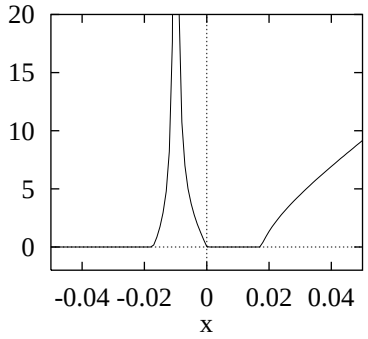

Figure 10: Lower bound for $|F(\mathbf{u}_\varepsilon(t,x))|$

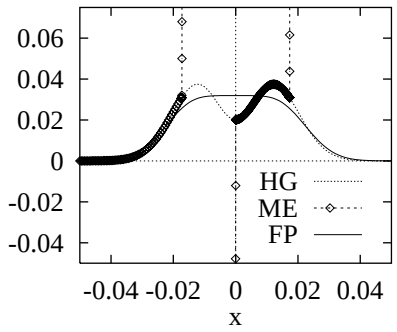

Figure 11: Comparison of fluxes

We find that, in those intervals where $s_\varepsilon < 0$, the GRAD flux $F^{lin}(\mathbf{u}_\varepsilon)$ (dotted line) practically coincides with the Maximum Entropy flux $F(\mathbf{u}_\varepsilon)$ (dashed line with

symbols). In view of the fact that the GRAD flux can be obtained by linearizing the Maximum Entropy flux in the region $s < 0$, this is not surprising. As soon as s_ε becomes positive, however, the Maximum Entropy flux diverges in contrast to the FOKKER PLANCK expression $u_{\varepsilon,5}$ (solid line). Note that the GRAD approximation stays reasonably close to $u_{\varepsilon,5}$. We remark that the calculation of $F(\mathbf{u}_\varepsilon(t,x))$ becomes increasingly hard the more $\mathbf{u}_\varepsilon(t,x)$ approaches the boundary E_5 of the domain of definition. In Fig. 12, the dashed line shows the representation of $\mathbf{u}_\varepsilon(t,x))$ for $t = 0.01$, $\varepsilon = 0.01$ and $x \in \mathbb{R}$ in the (q,s) diagram. The points where we have calculated the flux $F(\mathbf{u}_\varepsilon)$ are indicated by symbols.

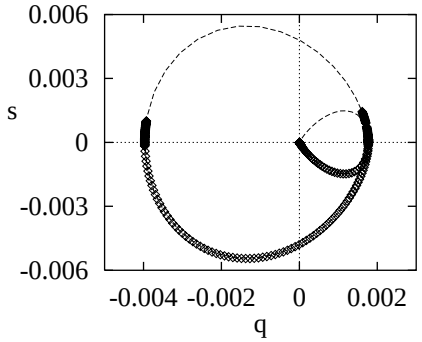

Figure 12: The flux F has been calculated at points with symbols

For the densely located points with symbols in the upper half plane, the calculations had to be carried out with up to 26 digits of accuracy (using MAPLE). Apart from the high accuracy requirements which rule out the use of standard programming languages for the flux evaluation, the calculations are extremely time consuming. For the evaluations at the points in the upper half plane, several days of computing time on a 500 MHz PC were required. Since any solution algorithm for the *Maximum Entropy system* requires flux evaluations, these observations indicate the expected difficulties in solving the *Maximum Entropy system* directly.

A comparison of the residues $\partial_x(F^{lin}(\mathbf{u}_\varepsilon) - (u_\varepsilon)_5)$ (dashed line with symbols) and $\partial_x(F(\mathbf{u}_\varepsilon) - (u_\varepsilon)_5)$ (dotted line) are given in Fig. 13.

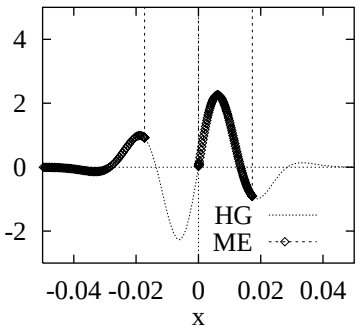

Figure 13: The residues

While the residue in GRAD's approach is still reasonable, the Maximum Entropy residue is much too large. This is observed by the very strong increase in the residue because of the large slopes of $F(\mathbf{u}_\varepsilon)$ in Fig. 11. Thus, the initial assumption of closeness between Maximum Entropy and FOKKER PLANCK solution is obviously not satisfied.

We compare the kinetic distribution functions, at the point $x = -0.017$ where the residues just start to differ strongly. In Fig. 14, we have depicted the distribution functions divided by the equilibrium density W^{eq} (without division, no major discrepancy is visible because of the exponential damping).

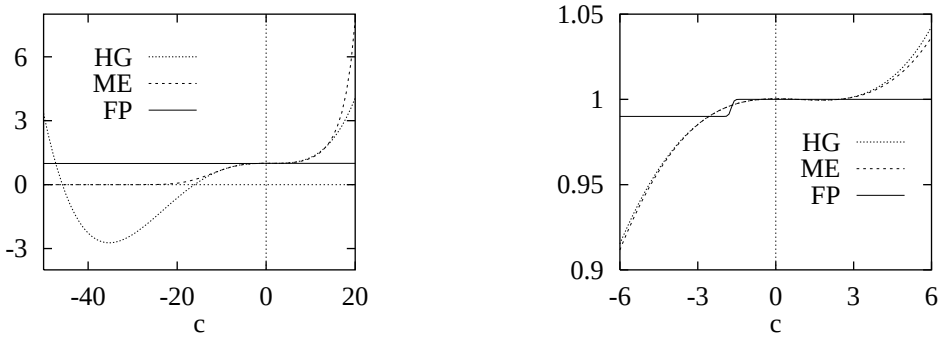

Figure 14: Comparison of scaled distribution functions

The FOKKER PLANCK solution is again given by the solid line, the HERMITE/GRAD distribution (30) is given by the dotted line and the Maximum Entropy distribution (21) is represented by a dashed line. Note that the HERMITE/GRAD distribution is not always positive and, for negative c, the Maximum Entropy distribution decays much faster than the Maxwellian. Also, for small $|c|$, the approximate distribution functions are very close to each other. To investigate the behavior at large positive c, we consider the logarithm of the distribution functions (see Fig. 15).

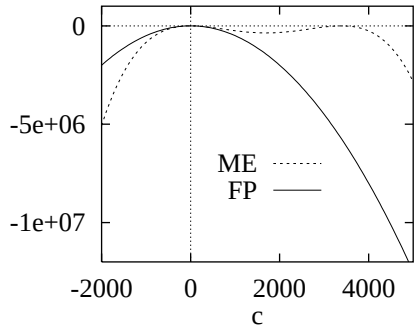

Figure 15: Comparison of logarithm of distribution functions

While the HERMITE/GRAD distribution now practically coincides with the exact distribution function, whenever the logarithm can be calculated, we find that the Maximum Entropy distribution develops a second peak around $c \approx 3400$ which is

not at all present in the FOKKER PLANCK solution. The importance of this peak on the moments can be estimated by calculating moment integrals of the Maximum Entropy distribution over the interval $[1700, \infty)$. We find the following normalized moments

moment	total	second peak
$\hat{u}_0$	1.000000	$1.02 \cdot 10^{-18}$
$\hat{u}_1$	0.000000	$3.48 \cdot 10^{-15}$
$\hat{u}_2$	1.000000	$1.18 \cdot 10^{-11}$
$\hat{u}_3$	0.017698	$4.01 \cdot 10^{-8}$
$\hat{u}_4$	3.000144	$1.36 \cdot 10^{-4}$
$\hat{u}_5$	0.478405	$4.61 \cdot 10^{-1}$

Obviously, there is very little mass related to the fast traveling particles and considerable contributions are found for the fourth and higher moments only. Note that the increase in the contribution from $\hat{u}_i$ to $\hat{u}_{i+1}$ is approximately a factor 3400 which is explained by the fact that the peak is located at $c \approx 3400$. A more detailed investigation shows that similar peaks show up whenever $s > 0$ and $s/|q|$ is sufficiently large. Obviously, the Maximum Entropy distribution function can only satisfy moment constraints with small q and large s (i.e. large ratio $s/|q|$) by introducing a peak at high velocities which contributes considerably more to the fourth moment s than to the third moment q. However, the contribution of the peak to the fifth moment is again considerably larger which eventually results in the singularity of the flux.

5 Conclusions

We have shown that problems with the Maximum Entropy approach for the FOKKER PLANCK equation arise if moments of order four and higher are used. The reason is that for such *Maximum Entropy systems*, the flux function is singular at equilibrium states. Since the singular behavior is lost in the linearization process, our **first conclusion** is that the linearized system is a bad approximation of the non-linear system in equilibrium states. However, it turns out that the linearized equations which happen to be equal to the HERMITE/GRAD system, are in much better coincidence with the FOKKER PLANCK equation in the sense that residues of exact solutions are much smaller than for the non-linear system. This observation leads to the **second conclusion** that the HERMITE/GRAD approach yields a better moment approximation than the Maximum Entropy approach. Combining the two conclusions, we have disproved the statement that the HERMITE/GRAD approach is just a linearization of the more powerful Maximum Entropy approach. In fact, the HERMITE/GRAD approach should be viewed as an independent method which is even favorable.

We also want to stress the fact that the form of the collision operator never entered explicitly in our investigations of the *Maximum Entropy systems*. This is due to the fact that the hyperbolic part in this system is completely determined by the form of the entropy functional and the moment functions $1, c, c^2, c^3, \ldots$. Hence, similar considerations apply to other kinetic equations like the BOLTZMANN equation of gas dynamics.

Our final comment concerns our restriction to a one-dimensional velocity space which has mainly been assumed for reasons of simplicity and clarity. If we consider the practically more important case of 14 moments in three space dimensions, we find similar problems: in this case, the set of inadmissible vectors $E_{14}^{(3)}$ forms a manifold of dimension 11 in the 14 dimensional, open, convex cone $K_{14}^{(3)}$ of moments of non-negative distribution functions. Again, the equilibrium points are located on the boundary of $E_{14}^{(3)}$. The bigger gap in dimension compared to the one-dimensional case is explained by the fact that a vanishing highest $\boldsymbol{\lambda}$-component (corresponding to $|\boldsymbol{c}|^4$) also forces the three previous components $\lambda_{10}, \lambda_{11}, \lambda_{12}$ to be zero (corresponding to $c_i|\boldsymbol{c}|^2$) to ensure integrability. The two extra constraints compared to the five-moment case in 1D where $\lambda_4 = 0$ only enforces $\lambda_3 = 0$, account for the lower dimension of the set of inadmissible moment vectors. Due to the bigger gap in dimension, it is less likely, that a generic moment vector is close to the singular boundary. This might be one of the reasons why the 14 moment system could be used for numerical simulations in [12]. Another reason might be that numerical simulations require approximate integration of the appearing integrals. If, for example, GAUSS-like integration rules are used, the contributions and problems due to the high velocities peaks in the Maximum Entropy distribution function are automatically suppressed. This, on the other hand, implies that numerical solutions obtained with such integration rules rather approximate the linearized system where the singular behavior is also suppressed.

Acknowledgements

W. Dreyer and M. Kunik gratefully acknowledge the support of the German Science Foundation under grant DR 401-2. M. Junk thanks the Weierstraß Institute for Applied Analysis and Stochastics (WIAS), where this work was started, for its very kind hospitality.

References

[1] G. Boillat, T. Ruggeri, *Moment equations in the kinetic theory of gases and wave velocities,* Cont. Mech. Thermodyn. **9**, No. 4 (1987), 205–212.

[2] S. Chandrasekhar, *Stochastic problems in physics and astronomy,* Reviews of Modern Physics **15**, No. 1 (1943), 2–87.

[3] W. Dreyer, *Maximization of the entropy in non–equilibrium*, J. Phys. A: Math. Gen., **20** (1987) 6505–6517.

[4] W. Dreyer, M. Kunik, *Initial and boundary value problems of hyperbolic heat conduction*, Cont. Mech. Thermodyn. **11**, No. 4 (1999) 227–245.

[5] W. DREYER, H. STRUCHTRUP, *Heat pulse experiments revisited.* Cont. Mech. Thermodyn. **5** (1993), 3–50.

[6] A. Einstein, *Eine neue Bestimmung der Moleküldimensionen*, Annalen der Physik **19** (1906), 289–306.

[7] A. Einstein, *Berichtigung zu meiner Arbeit: „Eine neue Bestimmung ...“*, Annalen der Physik **34** (1911), 591–592.

[8] H. Grad *On the kinetic theory of rarified gases*, Communications on Pure and Applied Mathematics **2** (1949), 311–407.

[9] S. Ihara, *Information Theory for Continuous Systems*, World Scientific, 1993.

[10] M. Junk, *Domain of Definition of Levermore's Five-Moment System*, J. Stat. Phys., **93** (1998) 1143-1167.

[11] M. Junk, *Maximum entropy for reduced moment problems*, Math. Models Methods Appl. Sci., accepted for publication.

[12] P. Le Tallec, J. P. Perlat, *Numerical analysis of Levermore's moment system*, Rapport de recherche No. 3124, INRIA Rocquencourt, 1997.

[13] C. D. Levermore, *Moment Closure Hierarchies for Kinetic Theories*, J. Stat. Phys. **83** (1996) 1021–1065.

[14] A. Majda, *Compressible fluid flow and systems of conservation laws in several space variables*, Springer, 1984.

[15] J. Meyer, J. Schröter, *Proper and normal solutions of the Fokker-Planck equation*, Arch. Rational Mech. Anal. **76** (1981) 193–246.

[16] I. MÜLLER, T. RUGGERI, *Rational Extended Thermodynamics.* 2nd Edition, Springer Tracts in Natural Philosophy, Springer New York, 1998.